Electrothermally actuated microelectromechanical systems based omega-ring terahertz metamaterial with polarization dependent characteristics

Chong Pei Ho, Prakash Pitchappa, Yu-Sheng Lin, Chia-Yi Huang, Piotr Kropelnicki, and Chengkuo Lee

Citation: Applied Physics Letters **104**, 161104 (2014); doi: 10.1063/1.4871999
View online: http://dx.doi.org/10.1063/1.4871999
View Table of Contents: http://scitation.aip.org/content/aip/journal/apl/104/16?ver=pdfcov
Published by the AIP Publishing

Electrothermally actuated microelectromechanical systems based omega-ring terahertz metamaterial with polarization dependent characteristics

Chong Pei Ho,[1] Prakash Pitchappa,[1] Yu-Sheng Lin,[1] Chia-Yi Huang,[2] Piotr Kropelnicki,[3] and Chengkuo Lee[1,a)]
[1]*Department of Electrical and Computer Engineering, National University of Singapore, 4 Engineering Drive 3, Singapore 117576, Singapore*
[2]*Department of Applied Physics, Tunghai University, No. 1727, Sec. 4, Taiwan Boulevard, Taichung 40704, Taiwan*
[3]*Excelitas Technologies, 8 Tractor Road, Singapore 627969, Singapore*

(Received 8 February 2014; accepted 8 April 2014; published online 21 April 2014)

We present the design, simulation, fabrication, and characterization of a continuously tunable Omega-ring terahertz metamaterial. The tunability of metamaterial is obtained by integrating microactuators into the metamaterial unit cell. Electrothermal actuation mechanism is used to provide higher tuning range, larger stroke, and enhanced repeatability. The maximum achieved tuning range for the resonant frequency is around 0.30 THz for the input power of 500 mW. This shows the potential of using electrothermally actuated microactuators based tunable metamaterial design for application such as filters, absorbers, sensors, and spectral imagers. © *2014 AIP Publishing LLC*. [http://dx.doi.org/10.1063/1.4871999]

Metamaterials have received intense attraction due to its ability to achieve electromagnetic (EM) properties which does not occur in nature.[1,2] Metamaterial is an array of sub-wavelength structures that can be designed to achieve specific EM properties and has diversified applications such as superlenses,[3–6] cloaking devices,[7] field enhancement,[8–10] and toroid responses.[11] More interestingly, the EM response of the metamaterial can actively controlled through external stimulus, which is of great significance in real time applications.[12] In order to realize tunability of metamaterials, typical methods employ the inclusion of a semiconductor diode to change the capacitance of the resonators media[13,14] or by changing the property of the surrounding media through optical, electrical, magnetic, or thermal means.[15–17] However, such tuning methods face a serious limitation in the tuning range and also an increased complexity in fabrication as the materials used are not CMOS compatible.[15,16] These limitations hinder the usage of tunable metamaterial in practical applications.

To overcome these drawbacks, microelectro-mechanical system (MEMS) techniques, which are well developed for the realization of three-dimensional movable structures in microscale, are integrated with metamaterial designs to achieve active tuning. Micromachined MEMS metamaterial has been demonstrated to display larger tuning range through electrostatic actuation by either changing the in-plane gap[18,19] or the structural layout of the unit cell.[20,21] However, electrostatic actuators suffer from pull-in phenomenon and so are not an ideal choice for continuously tunable metamaterial application. Thermal based actuation is of great potential as it offers larger stroke and higher repeatability. Tao *et al*. have reported thermally tunable MEMS metamaterials which consist of suspended silicon nitride plate with a single split-ring resonator (SRR) patterned on a gold film.[22] A pair of bimorph cantilevers is then used to support the SRR to complete the unit cell. Due to difference in the coefficient of thermal expansion (CTE) of silicon nitride and gold, when the device is heated using rapid thermal annealing (RTA), the bimorph cantilevers bend upwards and rotate the suspended metamaterial unit cell. However, the frequency tuning range presented is less than 0.02 THz and the maximum change in the transmission intensity is 45%. More importantly, the out-of-plane actuation of the device cannot be actively tuned and requires a RTA machine which is bulky. Similar thermal based actuation on the metamaterial unit cells is explored by Ou *et al*.,[23] where silicon nitride and gold are used to realize bimaterial bridges. To achieve bending of alternating bridges when heat is supplied, symmetric and asymmetric layer sequences are used. The experimental setup involved a heating stage and a maximum change of 50% in transmission was shown. Active control of the thermal actuation is, however, still not possible. This limitation decreases the feasibility of such devices in practical applications.

In this Letter, we present an electrothermally actuated microactuators integrated into an Omega-ring metamaterial unit cell to provide continuous tuning. Electrical current is used as the control signal to provide thermal energy to the movable microactuators through Joule heating. The continuous tuning range of 0.3 THz is experimentally achieved. The effect of current flow through the metamaterial, which leads to a temperature increase within the structure, and the spectral response to the incident THz waves are examined. The polarization dependent characteristics of the metamaterial are also studied which is important for the analysis of bi-anisotropic effects in Omega-ring metamaterial structures.[24,25]

Fig. 1(a) shows the top view of the unreleased metamaterial pattern shape which consists of an Omega-ring with an

a)Author to whom correspondence should be addressed. Electronic mail: elelc@nus.edu.sg.

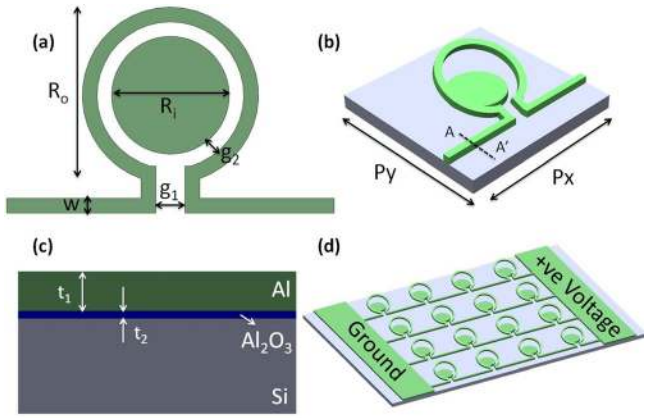

FIG. 1. (a) Design of Omega-ring metamaterial on the (b) unit cell. (c) Cross-sectional view of the device and (d) the Omega-ring metamaterial array with a metal line connecting the unit cells for MEMS operation.

inner disk. The feature size of the Omega-ring is chosen with the following parameters: unit cell pitch with Px and Py = 120 μm, outer ring radius $R_o = 60\,\mu$m, inner disk radius $R_i = 40\,\mu$m, beam width $w = 5\,\mu$m, $g_1 = 10\,\mu$m, and $g_2 = 5\,\mu$m. Fig. 1(b) shows the schematics of the metamaterial pattern with fixed central disk with released omega ring. The center of the inner disk coincides with the center of the unit cell.

Using purely CMOS compatible processes and materials, the metamaterial patterns are made of bimaterial layers—Al with a thickness t_1 of 500 nm on a thin layer of Al_2O_3 with a thickness t_2 of 40 nm as shown in Fig. 1(c).[20] In order to enable electrothermal actuation, continuous Al lines forming the released omega ring of the metamaterial are used to pass current when voltage is applied as shown in (d).

Fig. 2(a) shows the SEM image of the fabricated device. From the inset, the zoom-in image of the Omega-ring along with an inner disk design is more clearly shown. The released Omega-ring bends upwards with an angle of θ, as shown in Fig. 2(b), after the vapor hydrofluoric acid (VHF) release step due to the residual stress in Al_2O_3 and Al layers. When a potential difference is applied to the bond pads, a current will flow through the Al metal lines and the device will heat up due to Joule heating. This causes Al and Al_2O_3 to expand at different rate and since Al_2O_3 has a lower CTE relative to Al, the suspended structures will bend downwards with increasing temperature. The vertical displacement, δ, of the tip of the Omega-ring from the Si substrate can be estimated by the following equation:

$$\delta = \frac{3W_1W_2E_1E_2t_1t_2(t_1+t_2)(\alpha_2-\alpha_1)\Delta T \cdot L^2}{\begin{pmatrix}(E_1W_1{t_1}^2)^2+(E_2W_2{t_2}^2)^2\\ +\ 2W_1W_2E_1E_2t_1t_2(2{t_1}^2+3t_1t_2+2{t_2}^2)\end{pmatrix}}, \quad (1)$$

where subscript 1 and 2 refer to Al and Al_2O_3; W is the width; E is the Young's modulus ($E_1 = 70$ GPa and $E_2 = 530$ GPa); α refers to CTE ($\alpha_1 = 23.1 \times 10^{-6}$ K^{-1} and $\alpha_2 = 8.1 \times 10^{-6}$ K^{-1}); ΔT refers to the change in temperature; L is the length of the suspended beam.

To better understand the change in the EM properties of the Omega-ring metamaterial when electrothermally actuated towards the substrate, 3D finite-difference time-domain (FDTD) calculation is performed. In the simulations, the relative permittivity of Si and Al_2O_3 are set to 11.9 and 9.9, respectively. For Al, the permittivity, ε, is considered as a function of the resonant frequency ω. Using Drude-Lorentz's model,[26] ε can be estimated as

$$\varepsilon(\omega) = 1 - \frac{\omega_p^2}{\left(\omega^2 - \omega_{LC}^2 + i\Gamma\omega\right)}, \quad (2)$$

where ω_p is the plasma frequency, ω_{LC} is the resonant frequency, and Γ is a damping factor. In the simulations, TE-polarized incidence is defined with the electric field aligned to the y-axis and the magnetic field aligned to the x-axis. Conversely, in TM-polarized incidence, the electric field aligned to the x-axis and the magnetic field aligned to the y-direction.

As shown in Fig. 3(a), when the electric field is along the y-direction, i.e., TE-polarized incidence, the electric field at resonant frequency is coupled across the gap of the Omega-ring. Under TM-polarized incidence, the electric field is coupled across the gap between the omega-ring and the inner disk structure. As predicted by Aydin *et al.*,[25] the resonance frequency of TM-polarized incidence is higher than that of the TE-polarized incidence. This is shown in (c) and (d) where the resonance frequency of the device, when $\theta = 0°$, is 0.42 THz for TE-polarized incidence and 0.52 THz for TM-polarized incidence.

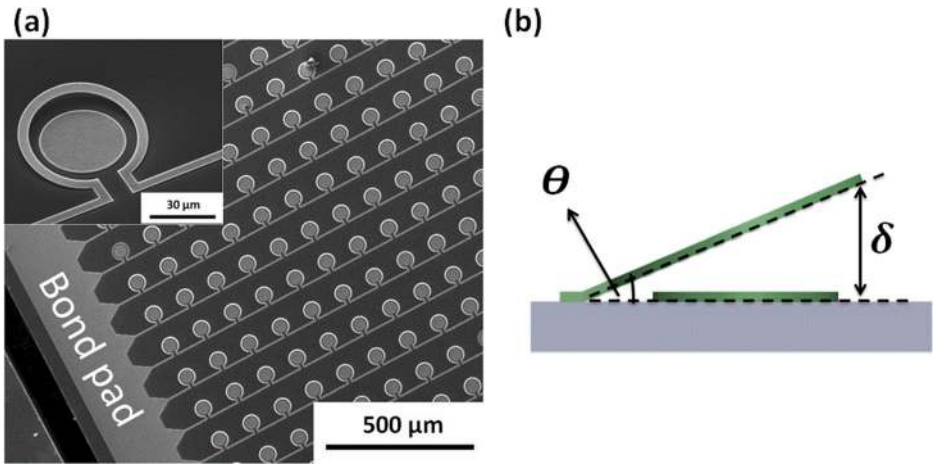

FIG. 2. (a) SEM image of the fabricated metamaterial device. The inset is the zoom-in image of the Omega-ring design and (b) cross-sectional view of released Omega-ring showing angle of curvature, θ, and bending height δ.

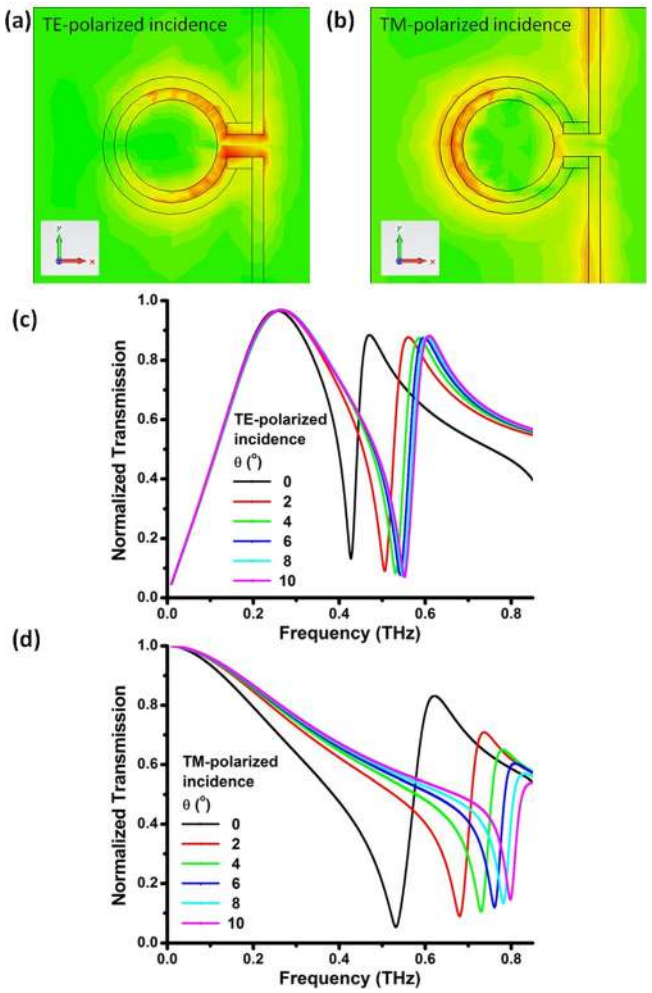

FIG. 3. Distribution of the electric resonance in the (a) TE-polarized incidence and (b) TM-polarized incidence. (c) and (d) are the simulated transmission spectra for different θ with TE-polarized incidence and TM-polarized incidence, respectively.

As mentioned above, after the Omega-ring part of the metamaterial unit cell is released, a current can be passed to induce electrothermal effects. Based on the analysis above, the Omega-ring will bend towards the substrate, thus decreasing θ in the process. By using different θ, an attempt is made to simulate the tunability of the device. It can be seen that the resonance frequency of the device decrease as θ decreases from 10° to 0°, where 10° is the initial state of the Omega ring after VHF release and 0° indicates a physical contact of the Omega-ring and the substrate. This resonant frequency of the metamaterial structure can be given as, $\omega = \sqrt{\frac{1}{LC}}$, where L and C refer to the effective inductance and capacitance in the metamaterial structure that enables coupling of the incident THz wave.[27–31] It can be quantitatively seen that as the Omega-ring bends towards the substrate, the gap between the metal and the substrate decreases. This increases the capacitance and hence the resonance frequency decreases.

Measurement of the EM response of the device for normal incident THz waves is done using TeraView TPS 300, which is a THz time domain spectroscopy (THz-TDS,) in its transmission mode. In all the measurements, the chamber is filled with nitrogen and the EM response is taken at room

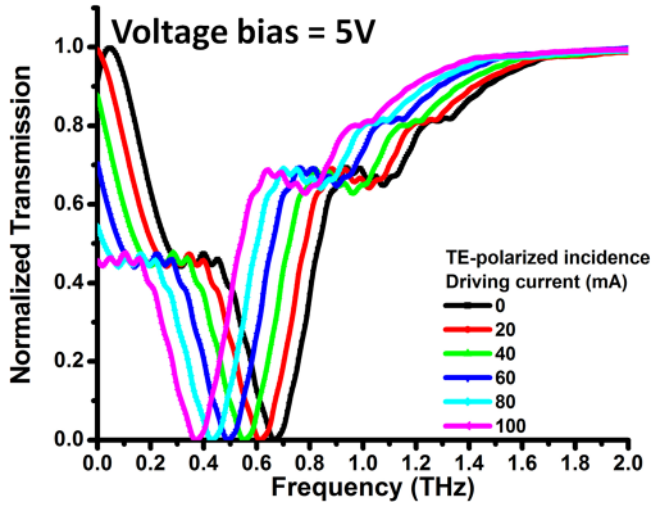

FIG. 4. Measured transmission spectra of Omega-ring metamaterial in the TE-polarized incidence response when the voltage bias is set to 5 V.

temperature. As shown in Fig. 4, for TE-polarized incidence response, the resonance frequency is around 0.67 THz when the Omega-ring is suspended after VHF release (10° case). This corresponds to a current supply of 0 mA. In order to actuate the released omega-ring, the input voltage was fixed at 5 V and the current was varied in steps of 20 mA. Continuous tuning is observed in the resonant frequency with respect to the input current. When the current is 100 mA, the resonant frequency is at 0.37 THz. After 100 mA, any increment of current does not change the transmission spectrum, hence, indicating that the Omega-ring is in physical contact with the substrate (0° case). For TM-polarized incidence as depicted in Fig. 5, the resonance frequency when the Omega-ring is suspended is slightly higher at 0.73 THz at 0 mA compared to the TE-polarized incidence case (0.67 THz at 0 mA). When the Omega-ring is heated using 100 mA of current and the physical contact is made with the substrate, the resonance frequency is shifted to 0.43 THz. In both TE-polarized incidence and TM-polarized incidence, it was demonstrated to have a tuning range of 0.30 THz. From the comparison with the

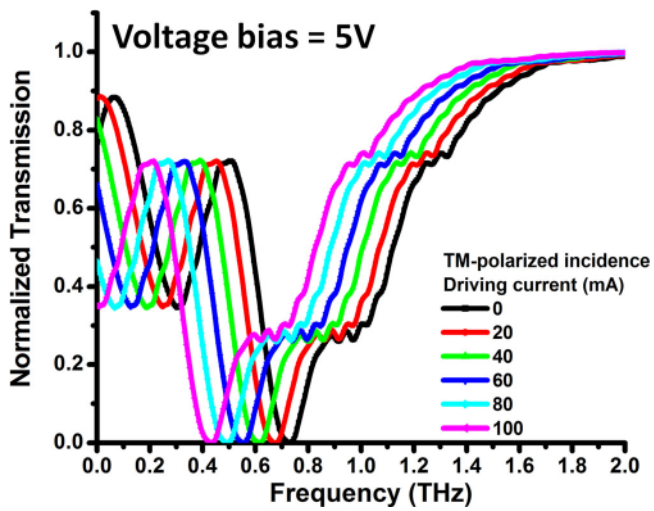

FIG. 5. Measured transmission spectra of Omega-ring metamaterial in the TM-polarized incidence when the voltage bias is set to 5 V.

simulation results, the Omega-ring metamaterial displays a more linear frequency shift. This can be attributed to the curvature of the Omega-ring after release which causes the Omega-ring to come into contact with the substrate gradually as current increases. The device is then cooled to room temperature and it is realized that the device is able to return to its original state, i.e., Omega-ring design being suspended over the substrate with an air gap between them. This highlights the repeatability of the device.

In order to study the effect of input current flowing through the metamaterial structures on the EM properties, electrostatic actuation was utilized to perform the tuning and the result is compared with the electrothermal case. For electrostatic actuation, a potential difference is applied between the Omega-ring and the substrate and there is no current flowing through the metamaterial structures. Similar to the concept shown by Lin *et al.*,[20] the electrostatic force produced will pull the suspended Omega-ring towards the substrate. When there is no bias difference between the bond pads and substrate, the Omega-ring is suspended freely and the device has a resonance frequency of 0.66 THz for TE-polarized incidence and 0.73 THz for TM-polarized incidence. As the DC bias difference increases, the suspended Omega-ring is pulled towards the substrate and hence θ decreases. At 25 V, the structure is snap-down and the resonance frequency shifts to 0.37 THz for TE-polarized incidence and 0.44 THz for TM-polarized incidence, indicating 0.30 THz tuning range for electrostatic actuation for both TE-polarized and TM-polarized incidence. Hence, the performance of the device when driven using electrostatic actuation is very similar to the case of electrothermal actuation. This shows that the introduction of DC current into the device and the high temperature induced in electrothermal actuation do not affect the EM response of the Omega-ring metamaterial. It is also noted that in electrostatic actuation, the device is not recoverable after coming into contact with the substrate. In electrothermal actuation, the device returns to its original state upon cooling down. This is a huge advantage of using electrothermal actuation as in the case of electrostatic the device can be tuned only once; however, in case of electrothermal, the repeatability of the device is much higher and hence more suitable in practical applications. At the same time, electrothermal actuation also offers larger stroke.

To characterize the polarization dependent characteristic of the Omega-ring metamaterial, another chip is released and its transmission spectra are measured with no input DC current. The input electric field and magnetic field are aligned with TE-polarized incidence as shown in the in the inset of Fig. 6. It is observed that when the device is not rotated, the resonance frequency is 0.67 THz. At a rotation angle of 45°, the device loses the TE-polarized incidence resonance characteristic and approaches the TM-polarized incidence resonance with an increase in the resonance frequency. At a rotation angle of 90°, the TM-polarized incidence resonance of the device is displayed.

In conclusion, a continuously tunable THz metamaterial design using electrothermal actuation is fabricated and demonstrated as a tunable THz filter. By using electrothermal actuation, the Omega-ring metamaterial has been shown to display a tuning range of 0.30 THz in both TE and TM-polarized incidence. The device also shows high repeatability and potentially large stroke. Electrostatic actuation is also experimentally studied and it displays very similar EM response as the results from electrothermal actuation. This shows that while harnessing the advantages of electrothermal actuation, the device did not face any limitation due to the high temperature induced or the DC current introduced during its operation. Electrothermal actuation also allows the device to recover to its original state after cooling. The polarization dependent state of the Omega-ring metamaterial is also characterized. This device also uses purely CMOS compatible processes and materials, with the innovation of using electrothermal actuation, is promising to many practical applications such as optical filters and sensors where large tuning range and high repeatability are desired.

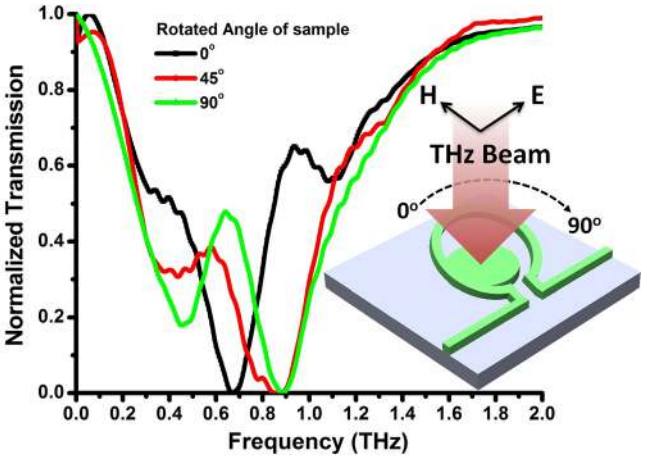

FIG. 6. Measured transmission spectra of Omega-ring metamaterial with TE-polarized incidence. The inset shows the schematic diagram of the device with different rotated angles.

The authors acknowledge the financial support from research grant of AcRF Tier 2-MOE2012-T2-2-154 at the National University of Singapore.

[1]H. J. Lezec, J. A. Dionne, and H. A. Atwater, Science **316**, 430 (2007).
[2]J. Valentine, S. Zhang, T. Zentgraf, E. Ulin-Avila, D. A. Genov, G. Bartal, and X. Zhang, Nature **455**, 376 (2008).
[3]N. Fang, H. Lee, C. Sun, and X. Zhang, Science **308**, 534 (2005).
[4]D. O. S. Melville and R. Blaikie, Opt. Express **13**, 2127 (2005).
[5]K. Aydin, I. Bulu, and E. Ozbay, New J. Phys. **8**, 221 (2006).
[6]Z. Liu, S. Durant, H. Lee, Y. Pikus, N. Fang, Y. Xiong, C. Sun, and X. Zhang, Nano Lett. **7**, 403 (2007).
[7]N. I. Zheludev, Science **328**, 582 (2010).
[8]R. Merlin, Appl. Phys. Lett. **84**, 1290 (2004).
[9]C. E. Talley, J. B. Jackson, C. Oubre, N. K. Grady, C. W. Hollars, S. M. Lane, T. R. Huser, P. Nordlander, and N. J. Halas, Nano Lett. **5**, 1569 (2005).
[10]E. Plum, K. Tanaka, W. T. Chen, V. A. Fedotov, D. P. Tsai, and N. I. Zheludev, J. Opt. **13**, 055102 (2011).
[11]T. Kaelberer, V. A. Fedotov, N. Papasimakis, D. P. Tsai, and N. I. Zheludev, Science **330**, 1510 (2010).
[12]N. I. Zheludev and Y. S. Kivshar, Nature Mater. **11**, 917 (2012).
[13]O. Paul, C. Imhof, B. Lägel, S. Wolff, J. Heinrich, S. Höfling, A. Forchel, R. Zengerle, R. Beigang, and M. Rahm, Opt. Express **17**, 819 (2009).
[14]Y. C. Jun and I. Brener, J. Opt. **14**, 114013 (2012).
[15]H.-T. Chen, W. J. Padilla, J. M. O. Zide, A. C. Gossard, A. J. Taylor, and R. D. Averitt, Nature **444**, 597 (2006).

[16]F. Zhang, L. Kang, Q. Zhao, J. Zhou, X. Zhao, and D. Lippens, Opt. Express **17**, 4360 (2009).
[17]A. D. Boardman, V. V. Grimalsky, Y. S. Kivshar, S. V. Koshevaya, M. Lapine, N. M. Litchinitser, V. N. Malnev, M. Noginov, Y. G. Rapoport, and V. M. Shalaev, Laser Photonics Rev. **5**, 287 (2011).
[18]W. M. Zhu, A. Q. Liu, W. Zhang, J. F. Tao, T. Bourouina, J. H. Teng, X. H. Zhang, Q. Y. Wu, H. Tanoto, H. C. Guo, G. Q. Lo, and D. L. Kwong, Appl. Phys. Lett. **99**, 221102 (2011).
[19]W. M. Zhu, A. Q. Liu, T. Bourouina, D. P. Tsai, J. H. Teng, X. H. Zhang, G. Q. Lo, D. L. Kwong, and N. I. Zheludev, Nat. Commun. **3**, 1274 (2012).
[20]Y. S. Lin, F. Ma, and C. Lee, Opt. Lett. **38**, 3126 (2013).
[21]F. Ma, Y. Qian, Y. S. Lin, H. Liu, X. Zhang, Z. Liu, M. L. Tsai, and C. Lee, Appl. Phys. Lett. **102**, 161912 (2013).
[22]H. Tao, A. Strikwerda, K. Fan, W. Padilla, X. Zhang, and R. Averitt, Phys. Rev. Lett. **103**, 147401 (2009).
[23]J. Y. Ou, E. Plum, L. Jiang, and N. I. Zheludev, Nano Lett. **11**, 2142 (2011).
[24]F. Zhang, G. Houzet, E. Lheurette, D. Lippens, M. Chaubet, and X. Zhao, J. Appl. Phys. **103**, 084312 (2008).
[25]K. Aydin, Z. Li, M. Hudlička, S. A. Tretyakov, and E. Ozbay, New J. Phys. **9**, 326 (2007).
[26]C. M. Soukoulis, M. Kafesaki, and E. N. Economou, Adv. Mater. **18**, 1941 (2006).
[27]M. Huang, J. Yang, J. Sun, J. Shi, and J. Peng, J. Infrared, Millimeter, Terahertz Waves **30**, 1131 (2009).
[28]L. L. Spada, F. Bilotti, and L. Vegni, Progress In Electromagnetics Research B **34**, 205 (2011).
[29]L. Yang, X. Shi, K. Chen, K. Fu, and B. Zhang, Physica B **431**, 11 (2013).
[30]F. Ma, Y. S. Lin, X. Zhang, and C. Lee, Light: Science & Applications **3**, e171, (2014).
[31]P. Pitchappa, C. P. Ho, Y. S. Lin, P. Kropelnicki, C. Y. Huang, N. Singh, and C. Lee, Appl. Phys. Lett. **104**, 151104 (2014).